



This is a repository copy of *Three-dimensional modelling of composite frames with ductile connections in fire*.

White Rose Research Online URL for this paper:

<https://eprints.whiterose.ac.uk/181867/>

Version: Accepted Version

---

**Article:**

Liu, Y., Huang, S.-S. and Burgess, I. (2022) Three-dimensional modelling of composite frames with ductile connections in fire. *Structures*, 36. pp. 665-677. ISSN 2352-0124

<https://doi.org/10.1016/j.istruc.2021.12.033>

---

Article available under the terms of the CC-BY-NC-ND licence  
(<https://creativecommons.org/licenses/by-nc-nd/4.0/>).

**Reuse**

This article is distributed under the terms of the Creative Commons Attribution-NonCommercial-NoDerivs (CC BY-NC-ND) licence. This licence only allows you to download this work and share it with others as long as you credit the authors, but you can't change the article in any way or use it commercially. More information and the full terms of the licence here: <https://creativecommons.org/licenses/>

**Takedown**

If you consider content in White Rose Research Online to be in breach of UK law, please notify us by emailing [eprints@whiterose.ac.uk](mailto:eprints@whiterose.ac.uk) including the URL of the record and the reason for the withdrawal request.



[eprints@whiterose.ac.uk](mailto:eprints@whiterose.ac.uk)  
<https://eprints.whiterose.ac.uk/>

# Three-Dimensional Modelling of Composite Frames with Ductile Connections in Fire

Yu Liu<sup>1\*</sup>, Shan-Shan Huang<sup>1</sup> and Ian Burgess<sup>1</sup>

<sup>1</sup> Department of Civil and Structural Engineering, University of Sheffield, Mappin Street, Sheffield S1 3JD, United Kingdom.

\* Corresponding Author: E-mail address: [yliu230@sheffield.ac.uk](mailto:yliu230@sheffield.ac.uk) (Yu Liu)

## Abstract

Connections are vital to the survival of steel and composite framed structures in fire. To prevent brittle failure of connections at elevated temperatures, a novel connection with high ductility has been proposed previously. In this paper, the fire performance of this ductile connection in composite frames is investigated. In order to consider the influence of the out-of-plane structural behaviour, the 3-D models of a fire compartment of a typical composite framed structure with different connection types, including the ductile connection, idealised rigid and pinned connections, as well as commonly used end-plate and web-cleat connections have been built using Vulcan to compare the performance of ductile connection with other connection types. Comparison results show that the proposed ductile connection can provide additional ductility within composite frame to accommodate the axial deformation of connected beam at high temperatures. To further save computational costs, the 3-D composite frame compartment model has been reduced to a quarter of its original size by using symmetric boundaries. The influence of unconnected length between the slab and beam on the connection performance has also been investigated. It is found that the relative beam end slip is affected by the unconnected length. However, due to the inherent mechanical properties of the ductile connection, the influence of unconnected length on the force of the ductile connection is negligible, which can also reflect the deformation capacity of ductile connection.

**Keywords:** Composite connection, Ductility, Component-based model, Fire, 3-D modelling

## 1. Introduction

Fire accidents occur frequently all over the world every year, causing huge casualties and property losses. Maintaining the integrity of buildings and preventing collapse in fire can provide valuable time for people to escape and for firefighters to extinguish the fire. Among all the structural elements in a steel framed building, connections are usually the weakest parts of a structure exposed to fire, and their failure can lead to the detachment of beams, collapse of floors, spreading of fire into other compartments and even the progressive collapse of the entire building.

1 However, traditional connection types lack axial ductility to accommodate the net expansion of beams during early  
2 heating and the net contraction of beams during the high-temperature “catenary” stage. In order to prevent the brittle  
3 failure of connections and improve the robustness of steel framed structures in fire, a novel connection with high  
4 axial deformability has been proposed by the authors [1-8]. A component-based model of the bare-steel ductile  
5 connection has been developed by the authors and incorporated into the software Vulcan [3-5]. 2-D bare-steel frames  
6 with ductile connections and other connection types have been modelled using Vulcan to compare their fire  
7 performance [4, 5]. The results show that, compared with conventional connection types, the ductile connection  
8 provides the additional ductility to accommodate the deformation of beams in fire, thus reducing the axial forces  
9 generated in connections and preventing connection failures.

10 Connection behaviour in composite structures in fire is significantly different from that in bare-steel structures,  
11 due to the continuity provided by the shear connection between the beams and concrete slabs. The thermal bowing  
12 of the floor system, caused by the fact that the composite slabs restrain the thermal expansion of the steel beams,  
13 affects the connection performance by generating high early-stage connection rotations. Leston-Jones [9, 10] carried  
14 out tests on composite end-plate connections under constant external load under increasing temperature, and  
15 obtained the moment-rotation relationships of end-plate connections across a realistic range of temperatures. Al-  
16 Jabri [11] conducted a series of high-temperature tests on flexible end-plate composite connections using a portable  
17 connection furnace. Based on his experimental results, a component-based model for the elevated temperature  
18 response of composite end-plate connections was proposed. Wellman et al. [12] investigated experimentally the  
19 structural behaviour of thin composite floor systems with two different connection types (welded-bolted fin-plate  
20 and all-bolted double-angle cleats) subject to combined gravity loads and fire loading. Li et al. [13] conducted three  
21 tests on flush end-plate composite joints at elevated temperatures and found that the rotational stiffness and moment  
22 capacity of composite joints are affected by the axial force from the restrained composite beam to which they are  
23 attached. They also proposed a simplified method to calculate the non-linear characteristics of composite  
24 connections in the analysis of beam catenary action at high temperatures, which was validated against their  
25 experimental results. Lin et al. [14] used 2-noded connection elements representing end-plate and partial-depth end-  
26 plate connections in their high-temperature 3-D composite floor model to take into account of the impact of  
27 connections on the 3-D behaviour of composite floors in fire. Selamet et al. [15] modelled a composite steel-framed  
28 floor system with beam-to-beam shear connections at elevated temperatures and found that the connection reaches  
29 its axial and rotational capacities during the fire cooling phase, leading to the failure of bolts caused by combined

1 shear and tension. Fischer et al. [16] built 3-D finite element models of composite beams with simple connections  
2 and carried out parametric studies to investigate the effect of connection type, deck type and slab reinforcement type  
3 on their structural response in fire. So far, the research on the fire performance of composite connections is still very  
4 limited. The performance of the ductile connection in bare-steel structures have already been well studied by the  
5 authors in previous papers [1-8]. It is necessary to study the high-temperature behaviour of the ductile connection  
6 in composite structures to verify whether the deformability of the ductile connection is still useful when used with  
7 composite floors.

8 The component-based model of the composite ductile connection has been developed by the authors by adding  
9 a rebar component to the bare-steel ductile connection model [6]. Isolated composite beam models with ductile  
10 connections were created to carry out parametric studies to investigate the influence of various parameters on the  
11 connection performance, including the connection thickness, the inner radius of the semi-cylindrical section and the  
12 number of longitudinal reinforcing bars within the effective width of the slab. However, structural elements in a  
13 composite steel-framed floor system always interact with each other and work as a whole. The influence of the out-  
14 of-plane structure, particularly slabs, on the connection performance cannot be accounted for by two-dimensional  
15 frame models including composite beams. Therefore, three-dimensional composite frame models have been built  
16 in this paper to investigate the connection behaviour. Limited research can be found on 3-D modelling of composite  
17 frames in fire conditions. Elghazouli et al. [17] created 3-D high-temperature grillage composite floor models using  
18 the non-linear numerical modelling software ADAPTIC, in which all the slabs, beams and columns were represented  
19 by cubic elasto-plastic beam-column elements. These models were validated against two of the Cardington full-  
20 scale fire tests. Lamont et al. [18] used Abaqus to simulate a small generic composite steel frame and compared the  
21 structural performance of the frame under two different single-floor compartment fire scenarios. Suwondo et al. [19]  
22 studied the progressive collapse of composite steel frames exposed to fire after earthquake, using a 3-D Abaqus  
23 composite building model, in which connection failures were not considered and all the connections were simplified  
24 either as ideally rigid or pinned.

25 Simulating a full 3-D composite frame in commercial finite element software (e.g. Abaqus) is extremely time-  
26 consuming, since it involves a huge number of elements and usually requires a dynamic explicit solver. In addition,  
27 to allow for reasonable computing times, most researchers had to use idealised connections when building 3-D  
28 composite frame models. Vulcan is a specialist software designed for high-temperature global frame analysis. It is  
29 capable of simulating the behaviour of 3-D composite structures at elevated temperatures, considering both

1 geometric and material non-linearities [20-23]. As mentioned previously, the component-based model of the  
2 composite ductile connection has been converted into a connection element, and incorporated into Vulcan. This  
3 component-based 2-noded connection element allows Vulcan to take into account the real behaviour of connections  
4 when modelling a composite frame, without high computational cost. It was, therefore, decided in this paper to use  
5 Vulcan to conduct the 3-D modelling in fire conditions.

6 This paper presents 3-D modelling of composite frames with ductile connections in fire. The geometric  
7 characteristics of the ductile connection, and its composite component-based model, will be introduced in detail. A  
8 single floor panel within a composite frame has been designed according to the typical frame layout adopted in the  
9 Cardington fire tests [24, 25]. The 3-D models of this composite frame compartment with different connection types,  
10 including the ductile connection, idealised rigid and pinned connections, as well as conventional end-plate and web-  
11 cleat connections, have been created using Vulcan. In order to further save computational cost, the 3-D composite  
12 frame compartment model has been reduced to a quarter of the original size by applying planes of symmetry at as  
13 many boundaries as possible. These models have also been used to investigate the influence of unconnected length  
14 between slab and beam on the connection performance in this research.

## 15 **2. The proposed ductile connection and the component-based model**

16 In order to improve the ductility of connections and enhance the robustness of structures in fire, a novel axially  
17 and rotationally ductile connection has been proposed by the authors [1-6]. This ductile connection consists of two  
18 identical parts, which can be manufactured by bending a steel plate. As shown in Figure 1 (a), each part of the  
19 ductile connection includes a fin-plate which is bolted to the beam web, a face-plate which is bolted to the column  
20 web or flange, and a semi-cylindrical section between the fin-plate and the face-plate. The semi-cylindrical section  
21 provides additional axial ductility by allowing the fin-plate to move towards or away from the face-plate by  
22 deforming plastically. Therefore, the diameter of the semi-cylindrical section is a critical parameter in the design of  
23 the ductile connection, and should be determined according to the ductility demand of the connected beam in fire.  
24 The authors have proposed a method to determine the axial deformations of the composite beam at four key positions  
25 during a fire event, including the rebar level, the connection's top and bottom surfaces, and the beam's bottom  
26 flange [6]. The diameter of the semi-cylindrical section should be larger than the greatest of the four axial  
27 deformations, to avoid hard contact within the connection, or between the beam bottom flange and the column  
28 flange. However, the diameter of the semi-cylindrical section should not be too large, otherwise, it may hinder the  
29 installation of bolts in the face-plate part of the connection, and may lead to hard contact between the semi-

1 cylindrical section and the end-plate. All other parameters, including the plate thickness, number of bolt rows and  
 2 height of connection section, can be determined according to EC3 [26].

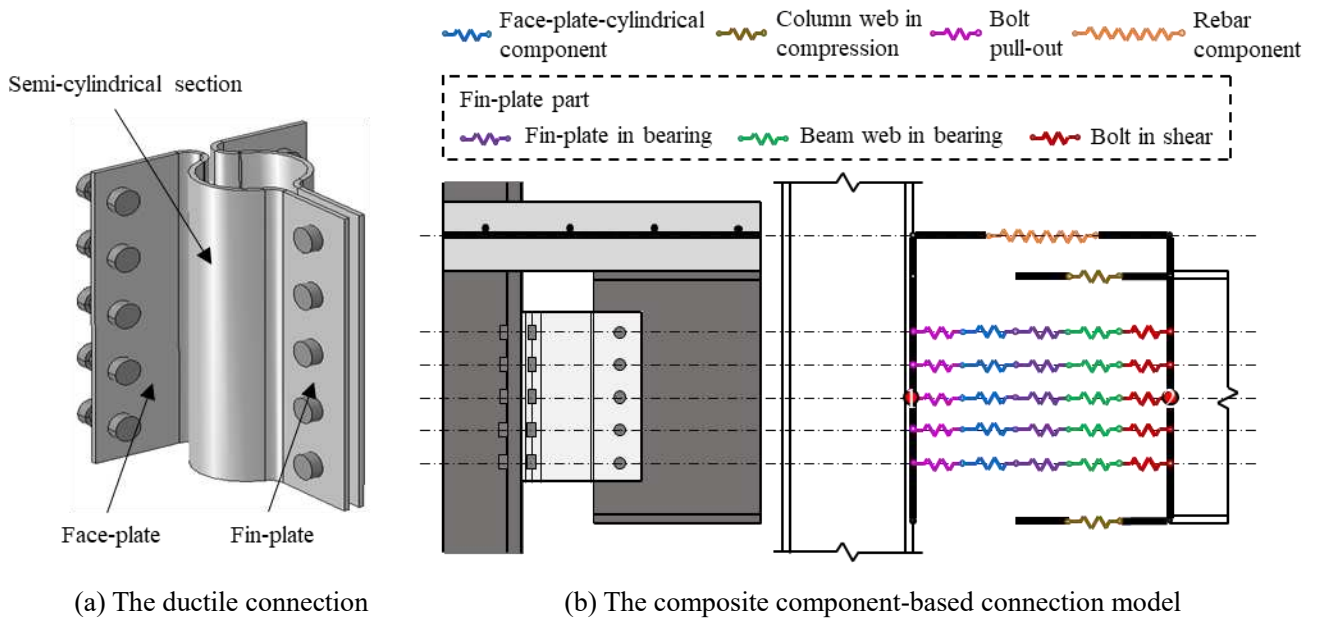


Figure 1. The proposed ductile connection and the component-based model

6 The component-based model of the bare-steel ductile connection has been developed by the authors [3], and  
 7 incorporated into the software Vulcan to facilitate global frame analyses [5]. A rebar component, which considers  
 8 the pull-out of reinforcing bars and the influence of weld points in the mesh, has been proposed and added to the  
 9 bare-steel component-based connection model to form the component-based model of the composite ductile  
 10 connection [6]. As shown in Figure 1 (b), the composite ductile connection model includes components representing  
 11 the face-plate-cylindrical section, column web in compression, bolt pull-out, rebar component, fin-plate in bearing,  
 12 beam web in bearing and bolt in shear. The gap between the compression spring row and the column flange is  
 13 designed to represent the maximum compressive displacement before internal contact occurs. The composite  
 14 component-based connection model has been incorporated into Vulcan and validated against a detailed Abaqus  
 15 model [6].

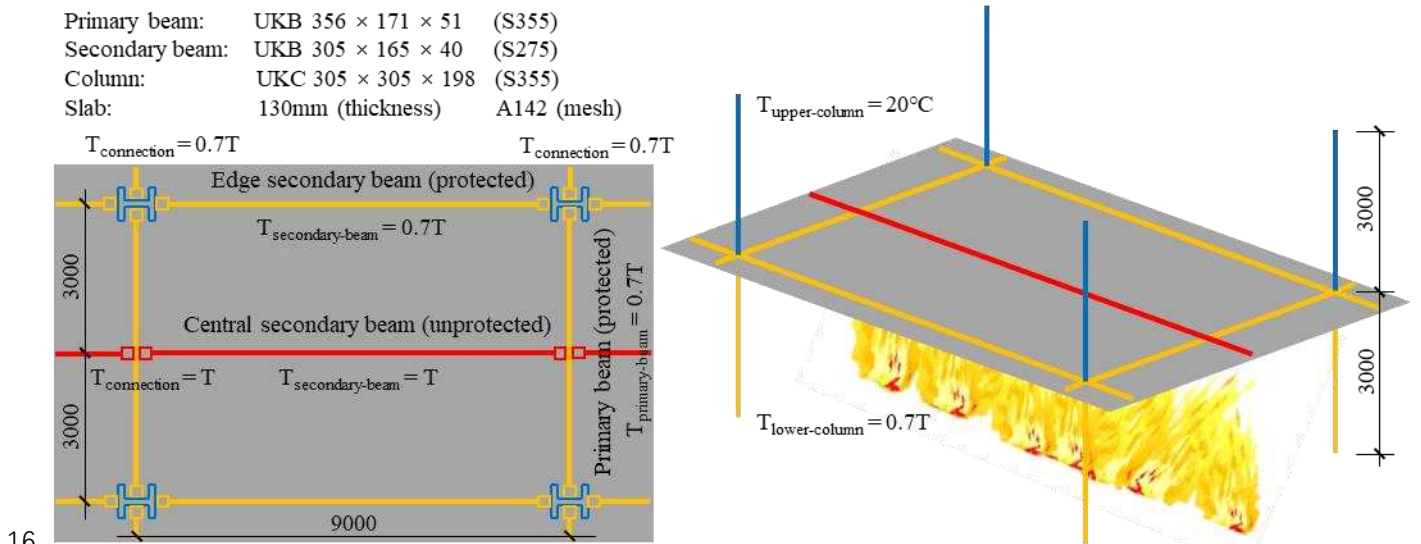
### 16 3. Comparison of the ductile connection with conventional connection types

17 Due to the contribution of composite slabs, the connection performance in a composite structure is very  
 18 different from that of a bare-steel structure. When building a composite frame model, the influence of the out-of-  
 19 plane structure on the performance of the composite connections must be taken into consideration. In this section,  
 20 3-D composite frame models with different types of connections are created using Vulcan to compare the

1 performance of ductile connection with other connection types.

### 2 **3.1 3-D composite frame model**

3 On the basis of the typical frame structure adopted in the Cardington full-scale fire tests [24, 25], an internal  
4 compartment of a composite frame is designed as shown in Figure 2. The sections adopted for primary and  
5 secondary beams are selected as UKB 356 × 171 × 51 and UKB 305 × 165 × 40, respectively. The column section  
6 is selected as UKC 305 × 305 × 198. The thickness of the composite slab is 130 mm and A142 mesh is adopted. It  
7 should be noted that the composite connection element already includes rebar component, therefore the slab  
8 elements above the connections in the models do not contain reinforcement to avoid repetition. It is assumed that  
9 fire occurs on the lower floor, including beneath adjacent floor panels. The beams on the column grid and the  
10 columns themselves are protected to the same level, whereas the central secondary beam is unprotected. The  
11 temperatures of all the gridline beams and lower columns are set to 70% of the central secondary beam's temperature,  
12 and the upper columns remain at ambient temperature. The temperature of each connection is equal to the  
13 temperature of the beam to which it is connected. Taking the permanent load as 3.65 kN/m<sup>2</sup> and the imposed load  
14 as 3.5 kN/m<sup>2</sup>, the combined load applied on the slab in the fire limit state should be 3.65+3.5×0.5=5.4 kN/m<sup>2</sup>. The  
15 detailed dimensions of the ductile connections used in the composite frame are shown in Figure 3.



17 Figure 2. Design of the internal compartment of a composite frame (unit: mm)

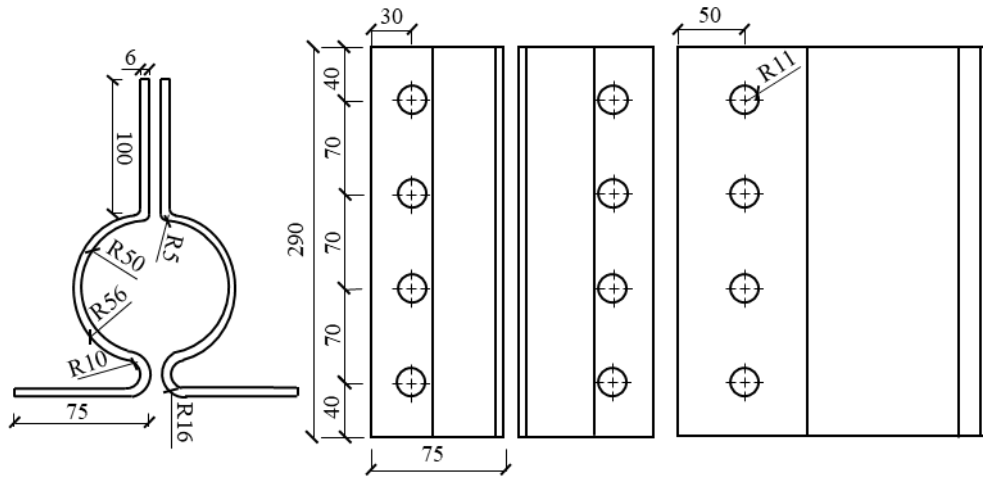
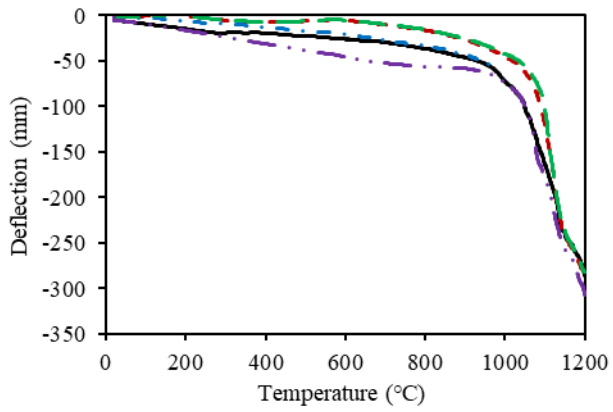


Figure 3. Detailed dimensions of the ductile connection (unit: mm)

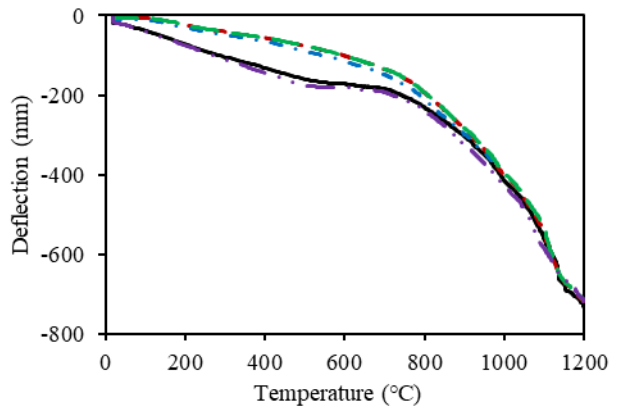
### 3.2 Comparison of the ductile connection with other connection types

The 3-D composite frame models (Figure 2) with different types of connections, including ideally pinned and rigid connections, and the conventional end-plate and web-cleat connections, have been created using Vulcan to compare the structural performance using these connection types. Full shear connection is assumed between the slab and beams, and this is modelled by sharing the nodes between the slab and beam elements. To save computational cost, only a half of the models is built, and planes of symmetry are applied to the boundaries of each model. The component-based models of bare-steel end-plate connections and bare-steel web-cleat connections have already been incorporated into Vulcan by Block [27] and the authors [5], respectively. Rebar components have now been added to these two models, to model the whole composite joint zone including either end-plate connections or web-cleat connections. The results of the comparison are shown in Figure 4 (a) - (c), which shows that altering the connection type has little effect on the mid-span deflections of the primary, central secondary and edge secondary beams. At the same temperature, the deflections of the beams with ductile connections and ideally pinned connections are generally larger than those of the beams with the other connection types. Compared with the other connection types, the axial forces generated in the ductile connections are considerably reduced, as shown in Figure 4 (d) - (f). This indicates that the proposed ductile connection can provide satisfactory deformability to accommodate the axial displacement applied by the connected beam in fire without increasing axial force levels markedly.



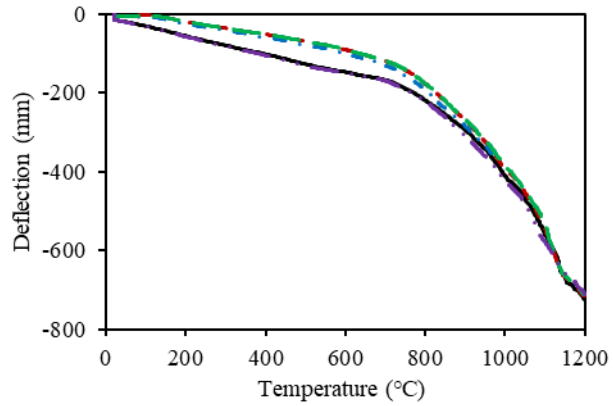
— Ductile connection      - - - End-plate connection  
 - · - web-cleat connection      - - - Rigid connection  
 - · · Pinned connection

(a) Mid-span deflection of primary beam



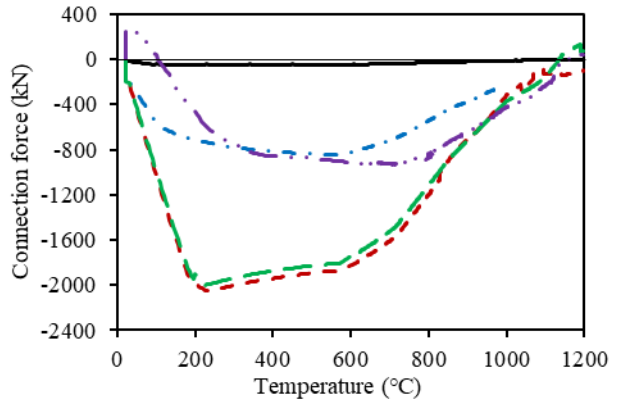
— Ductile connection      - - - End-plate connection  
 - · - web-cleat connection      - - - Rigid connection  
 - · · Pinned connection

(b) Mid-span deflection of central secondary beam



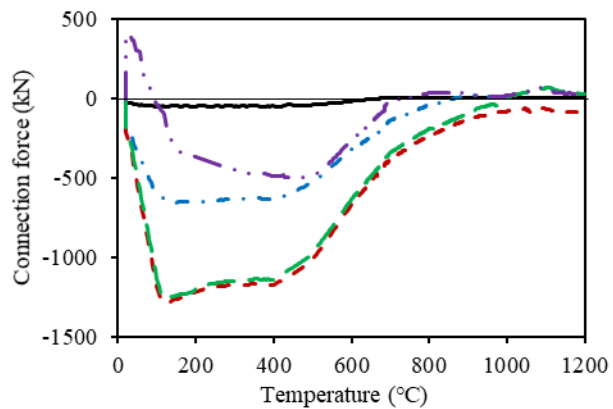
— Ductile connection      - - - End-plate connection  
 - · - Web-cleat connection      - - - Rigid connection  
 - · · Pinned connection

(c) Mid-span deflection of edge secondary beam



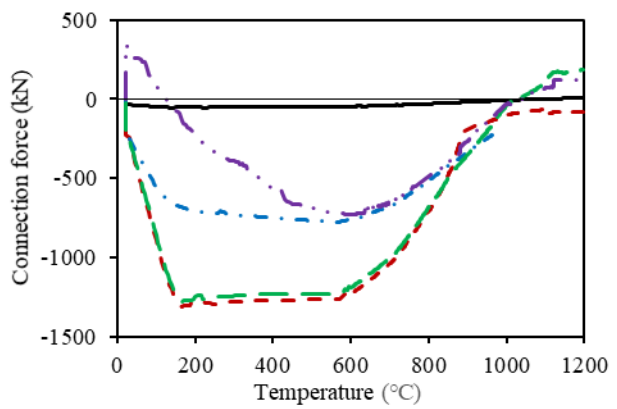
— Ductile connection      - - - End-plate connection  
 - · - Web-cleat connection      - - - Rigid connection  
 - · · Pinned connection

(d) Primary beam-to-column connection force



— Ductile connection      - - - End-plate connection  
 - · - Web-cleat connection      - - - Rigid connection  
 - · · Pinned connection

(e) Central secondary beam-to-primary beam connection force



— Ductile connection      - - - End-plate connection  
 - · - web-cleat connection      - - - Rigid connection  
 - · · Pinned connection

(f) Edge secondary beam-to-column connection force

1

2

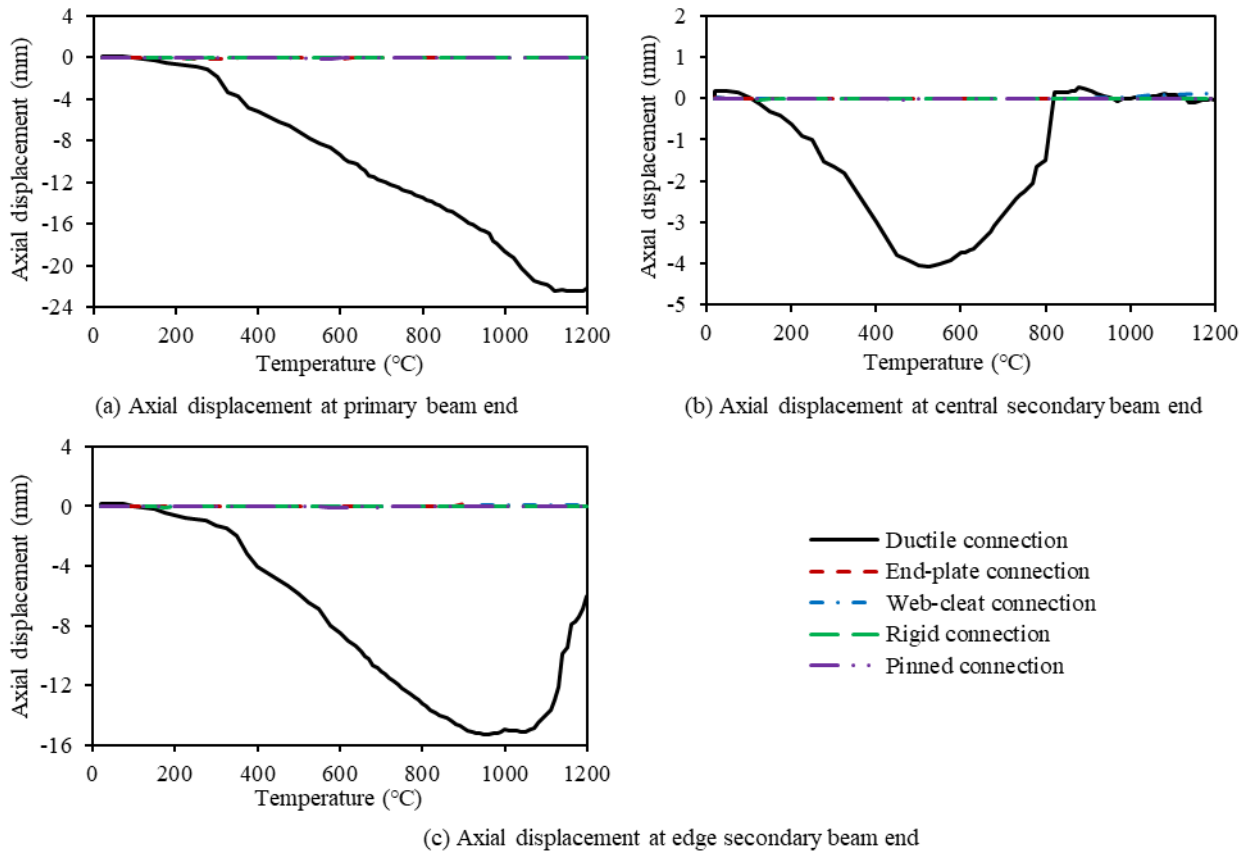
3

4

Figure 4. Comparative results (the abscissas of all the subfigures are the temperature of the unprotected central secondary beam)

In order to further illustrate the deformation capacity of the ductile connection, the axial displacements at the ends

1 of beams with different connection types are compared and shown in Figure 5. In this figure, the negative value  
2 represents compressive displacement, and the positive value represents tensile displacement. It is obvious that the  
3 axial displacements at the beam ends with ductile connections are much larger than those of the other connection  
4 types, and their values are not even of the same order of magnitude. Looking at the development of the axial  
5 displacements at beam ends with ductile connections as temperature increases, the observed increase in the  
6 compressive displacements at the beam ends are probably mainly due to the thermal expansion of the steel beam.  
7 When the temperature of the central secondary beam exceeds 500 °C, the increase in beam curvature caused by the  
8 reduced steel strength compensates for the compressive displacement at beam end, resulting in a decrease of the  
9 compressive displacement, as shown in Figure 5 (b). At around 800 °C, the axial displacement at the end of the  
10 central secondary beam becomes tensile, indicating that the beam is entering the catenary action stage. After this  
11 stage, the tensile axial displacement of the central secondary beam basically remains unchanged and does not  
12 continue to increase. It is well known that, at 800°C, the strength of steel has dropped to about 10% of its original  
13 strength, and the steel beam has lost most of its flexural load carrying capacity. In this model, the slab is assumed  
14 to be kept at ambient temperature, and the concrete has some tensile strength, albeit very low. Therefore, the external  
15 load originally borne by the central secondary beam is now largely taken by the tensile membrane action of the  
16 concrete slab, and so the tensile axial displacement of the central secondary beam does not increase further. The  
17 edge secondary beam is protected, so its axial displacement decreases much later than that of the central secondary  
18 beam. Since the section size of the primary beam is relatively large, and its span is relatively short compared with  
19 the secondary beams, the compressive displacement at the end of the primary beam keeps increasing during the  
20 whole analysis.

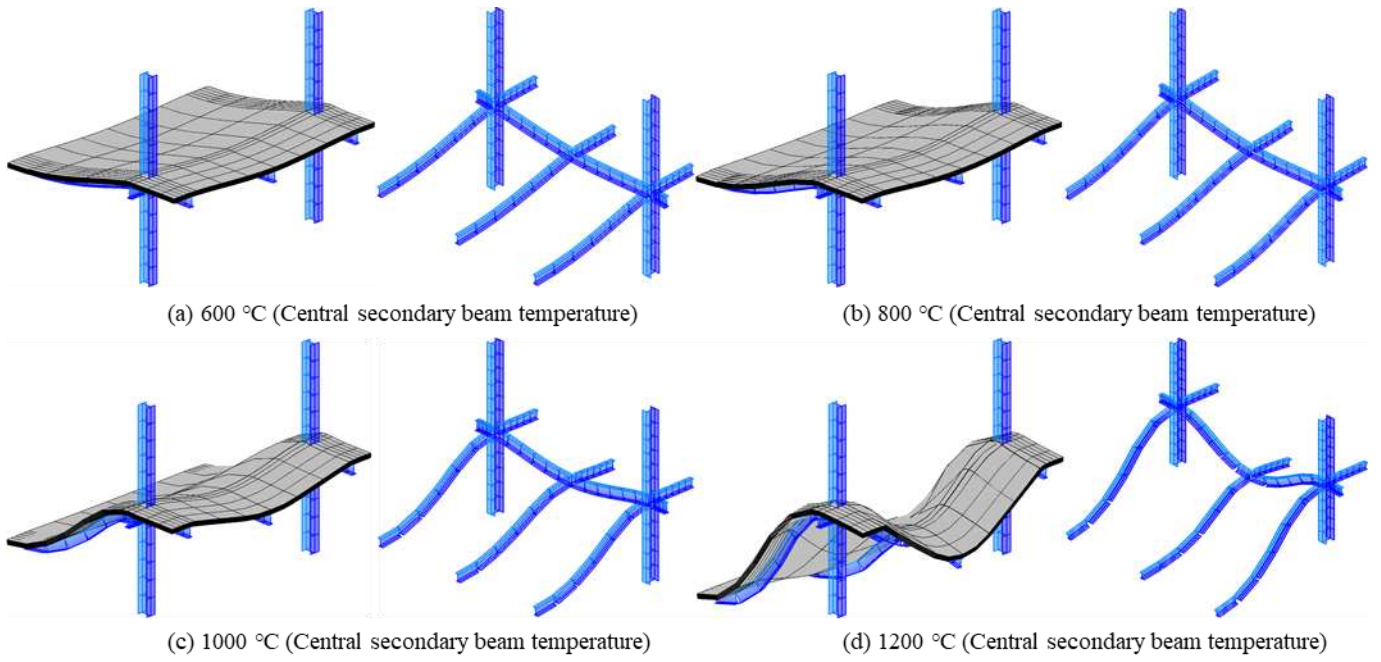


1 (c) Axial displacement at edge secondary beam end

2 Figure 5. Axial displacements at beam ends (the abscissas of all the subfigures are the temperature of the  
3 unprotected central secondary beam)

4 The deformation of the 3-D composite frame model with ductile connections is shown in Figure 6. This figure  
5 shows that the ductile connection can provide very high axial ductility, thus accommodating the net contraction of  
6 the beam during the high-temperature catenary stage, without fracturing the connection. Figure 7 - Figure 9 illustrate  
7 the force-temperature and displacement-temperature curves for each spring row and rebar component of the primary  
8 beam-to-column connection, the central secondary beam-to-primary beam connection, and the edge secondary  
9 beam-to-column connection. It is shown in Figure 7 that, until about 1100 °C, the primary beam has been in the  
10 thermal expansion stage, and the compressive displacement of each spring row of the primary beam connection  
11 continues to increase. Compared with the primary beam, the edge secondary beam has a smaller cross section and  
12 a longer span. Therefore, the edge secondary beam enters the catenary action stage at a lower temperature (around  
13 900 °C) compared to the primary beam. The compressive displacement of each spring row begins to decrease after  
14 exceeding this temperature, as shown in Figure 8. The central secondary beam is designed to be unprotected, and  
15 has a higher temperature than the other beams, resulting in its entering the catenary action stage at a lower  
16 temperature compared with the edge secondary beam. At around 700 °C, the force in each spring row of the central

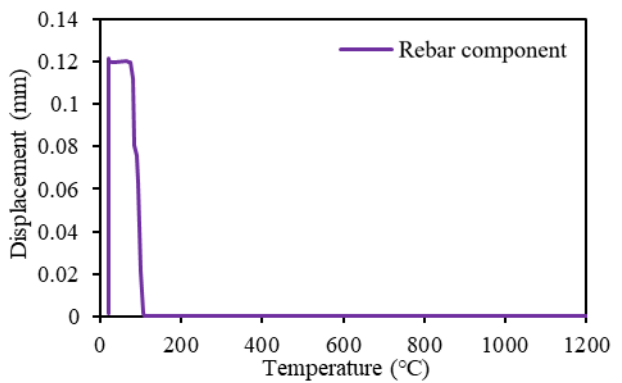
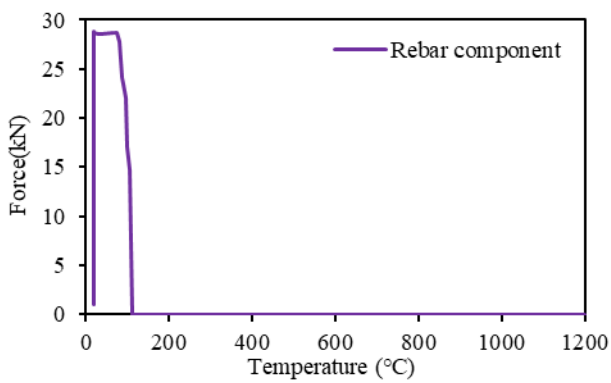
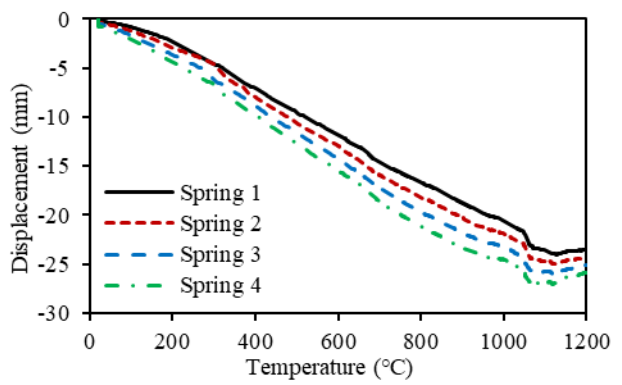
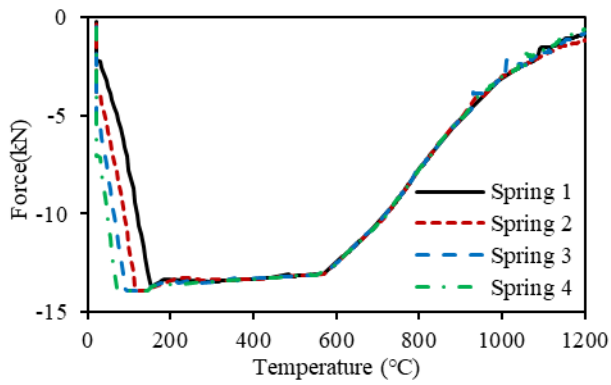
1 secondary beam connection becomes tensile, indicating that this spring row has entered the ‘pulling-back’ stage [3].  
2 The ‘pulling-back’ stage refers to the pre-compressed connection being pulled back towards its original state as  
3 each spring row is gradually pulled back towards its original length. During this period, the tensile force in each  
4 spring row also gradually decreases, due to the degradation of the connection’s material properties as its temperature  
5 rises. The displacement of the rebar component in Figure 7 (d), Figure 8 (d) and Figure 9 (d) represents the crack-  
6 width of the concrete slab above the connection, which is determined by the rebar type (the development length of  
7 rebar), the weld-point locations of the mesh and the position of the crack [6]. In the connection element, the  
8 displacements and rotations of the two connection element nodes are used to determine the axial separation at the  
9 rebar level under the plane section assumption, and the rebar component is only activated under tension. Figure 7  
10 (d), Figure 8 (d) and Figure 9 (d) show that the rebar components of all the three connections are temporarily  
11 activated below 100 °C due to the hogging moment applied to the connection. Beyond this point, the rebar  
12 components of the primary beam and edge secondary beam connections remain inactive, since the beam’s thermal  
13 expansion compensates for the tensile displacement of the rebar component, whereas the rebar component of the  
14 central secondary beam connection is activated again at about 800 °C. This confirms that the neutral axis of bending  
15 moves during a fire event, as expected. At ambient temperature, the neutral axis of bending is below the rebar. It  
16 then moves upward with the increase of temperature in the initial heating stage. When the beam enters the catenary  
17 action stage at very high temperatures, the beam has lost most of its bearing capacity and the neutral axis moves  
18 below the rebar again, causing the rebar component to be re-activated. In general, compared with other types of  
19 connection, the ductile connection exhibits considerable axial deformability in composite frames, which can  
20 significantly reduce the forces generated in the connections and prevent premature fracture of connections in fire.



1

2

Figure 6. Deformations of the 3-D composite frame model (central secondary beam temperature)

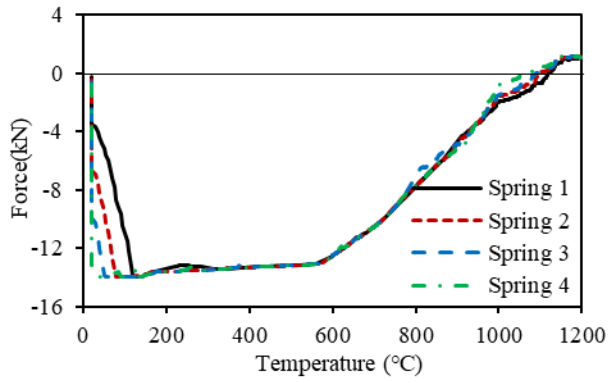


3

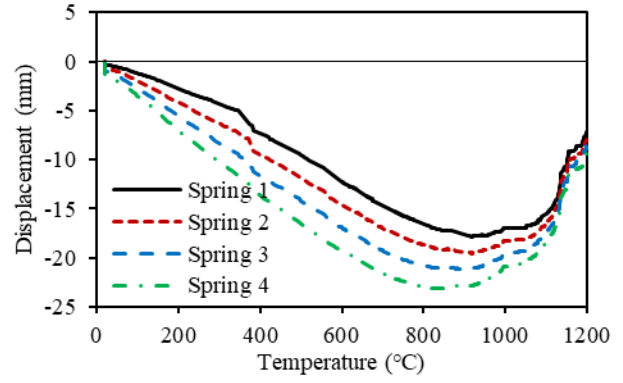
4

5

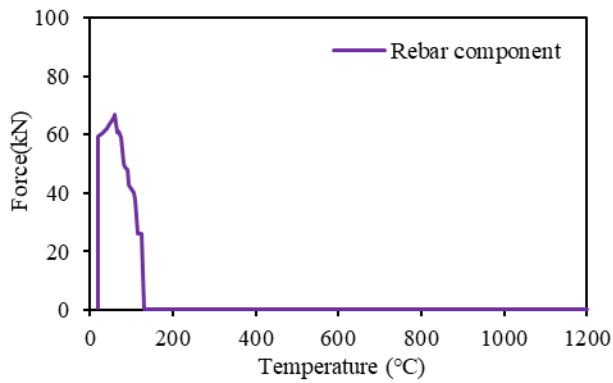
Figure 7. Primary beam-to-column connection (the abscissas of all the subfigures are the temperature of the unprotected central secondary beam)



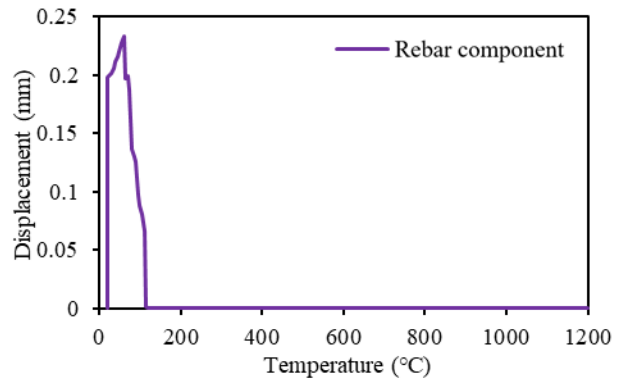
(a) Force-temperature curve of each spring row



(b) Displacement-temperature curve of each spring row



(c) Force-temperature curve of rebar component



(d) Displacement-temperature curve of rebar component

1

2

3

Figure 8. Edge secondary beam-to-column connection (the abscissas of all the subfigures are the temperature of the unprotected central secondary beam)

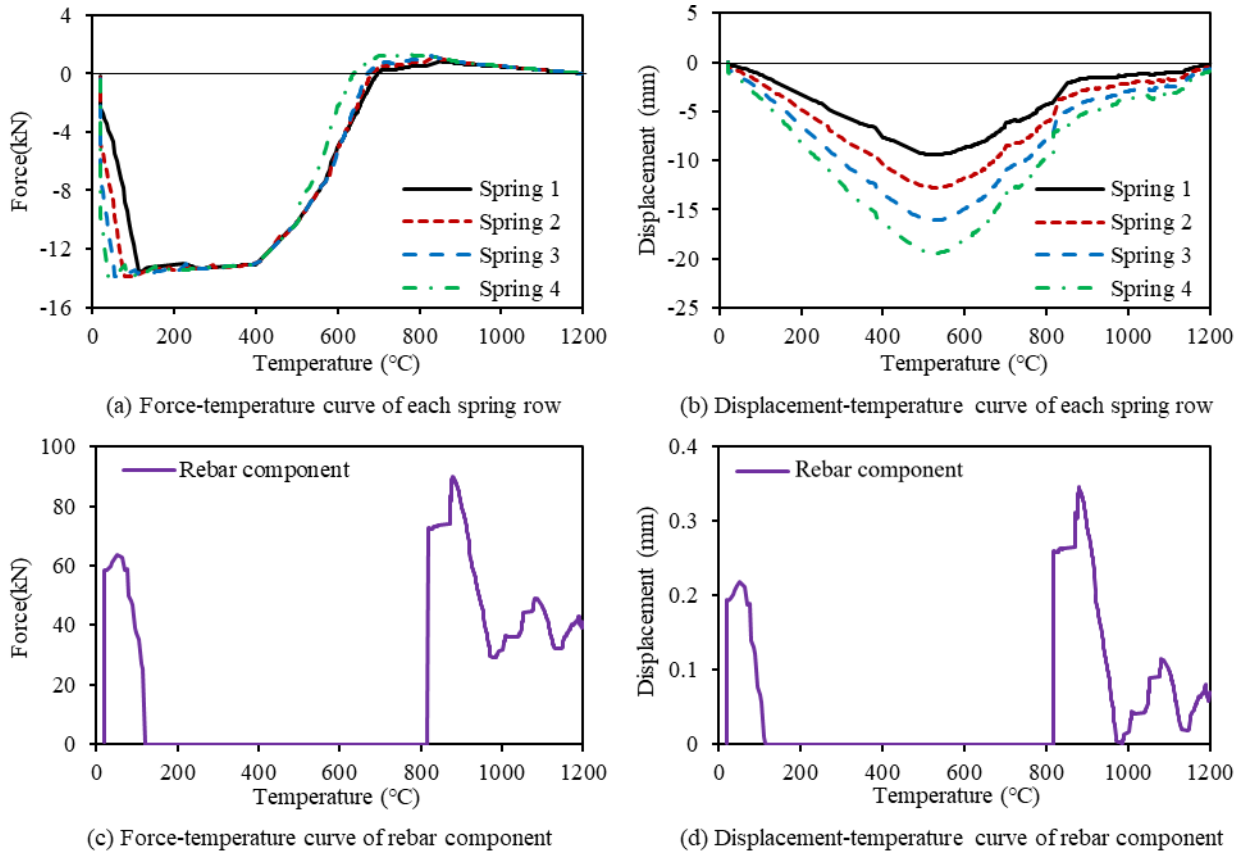
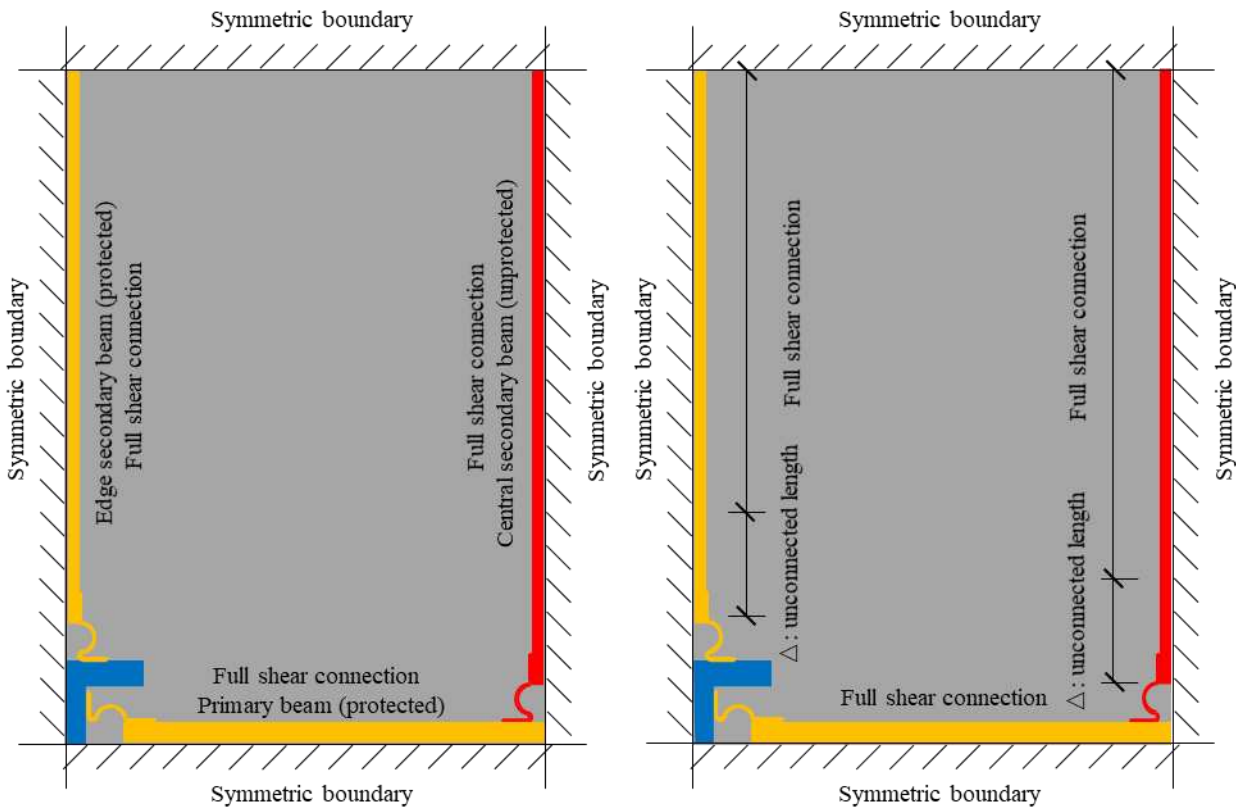


Figure 9. Central secondary beam-to-primary beam connection (c the abscissas of all the subfigures are the temperature of the unprotected central secondary beam)

#### 4. Influence of distribution of shear studs on connection performance

Shear studs are usually uniformly distributed along a beam span. The maximum sagging moment usually occurs at the mid-span, whereas the maximum relative slip between the steel section and slab occurs at the beam ends. Therefore, if the shear studs are concentrated in the central zone of the beam span, allowing the steel beam to move freely relative to the slab at its ends, it might be expected that the thermal bowing deformation of the composite beam would be reduced. It might also be expected that the end slip would increase (negatively), but this should easily be accommodated by the ductile connection without generating a large axial force. In order to verify this idea, the 3-D composite frame model shown in Figure 2 is used in this section to investigate the impact of the shear stud distribution on the performance of the composite ductile connection. The 3-D model shown in Figure 2 is a large model of a huge number of elements, which takes nearly a month to run. It was, therefore, decided to build a quarter of the original model and apply planes of symmetry at the boundaries, as shown in Figure 10. The section sizes of the primary, edge secondary, and central secondary beams, the column and connections remain unchanged. It should

1 be noted that due to the boundary conditions applied, only half of the beam and connection sections, and a quarter  
 2 of the column section, are included in the actual model. Taking full shear connection as the control case (Figure 10  
 3 (a)), the shear studs of all secondary beams are concentrated in the central zone of the beam span in the comparative  
 4 models with different unconnected lengths  $\Delta$ . These are 250 mm, 500 mm, 1000 mm, and 1500 mm, as shown in  
 5 Figure 10 (b). The primary beams in all models are fully shear-connected, since the primary beam is protected and  
 6 has shorter span and larger section compared with the secondary beams.



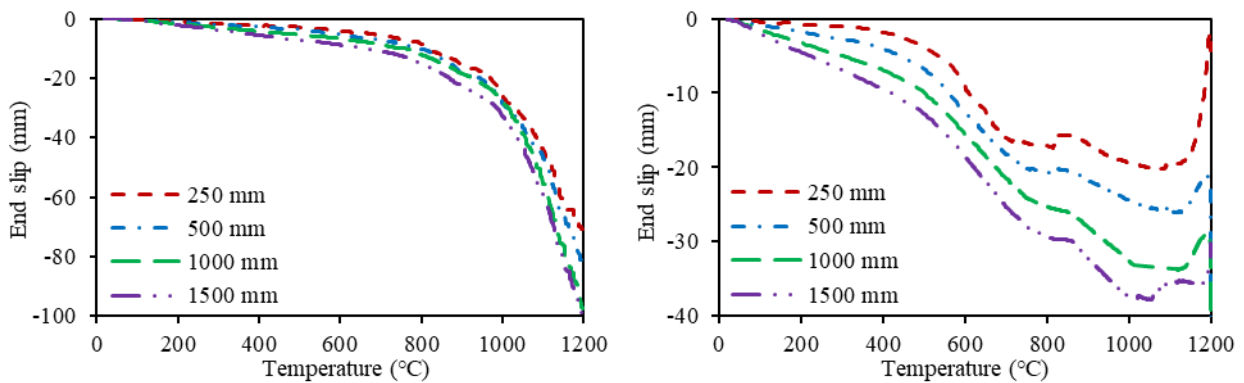
7 (a) Full shear connection model

8 (b) Model with a certain length of beam and slab unconnected

9 Figure 10. Models with different unconnected lengths

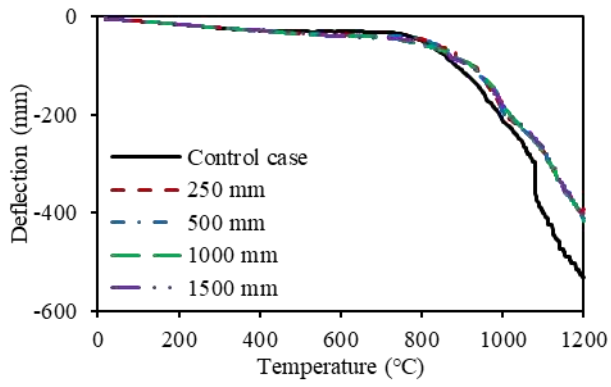
10 It is to be expected that the longer the unconnected length of the beam, the larger the relative slip at the beam  
 11 end. Figure 11 shows that the effect of the unconnected length on the end slip is negligible in the edge secondary  
 12 beam, whereas, it is very obvious in the central secondary beam. At a certain temperature, the central secondary  
 13 beam of the largest unconnected length (1500mm) experiences the largest negative end slip among all the central  
 14 secondary beams analysed. Note here that the end slip is negative when the beam end moves towards the column  
 15 relative to the slab. As the temperature rises to about 1000 °C, the negative end slip begins to decrease, indicating  
 16 that the beam is beginning to move away from the column as it enters the catenary action stage. The comparative  
 17 results of the models with different unconnected lengths are shown in Figure 12. This figure shows that the mid-

1 span deflections and the axial connection forces of the primary beam, the edge secondary beam and the central  
 2 secondary beam are only slightly affected by the unconnected length. Figure 11 (a) shows that the edge secondary  
 3 beams with different unconnected lengths generate almost the same end slip. It should be noted that the primary  
 4 beams in all models are fully connected to the slab. Therefore, it is reasonable to conclude that the distribution of  
 5 shear studs along the secondary beam has little effect on the behaviour of the primary beam and the edge secondary  
 6 beam. As for the central secondary beam, different unconnected lengths do generate different relative slip at the  
 7 beam end (Figure 11 (b)), whereas the connection axial force is not significantly affected. The reasoning behind this  
 8 is illustrated in Figure 13. This figure shows the force-displacement curves of a spring row of the ductile connection  
 9 at different temperatures, indicating that, at a certain temperature, the compressive force of the spring row reaches  
 10 its peak value soon after it enters compression. After passing its peak, the curve remains almost horizontal until the  
 11 maximum compressive displacement is reached, at which internal contact occurs within the semi-cylindrical section.  
 12 Therefore, even though different end slips are applied to the connections, the connection axial forces are almost the  
 13 same.

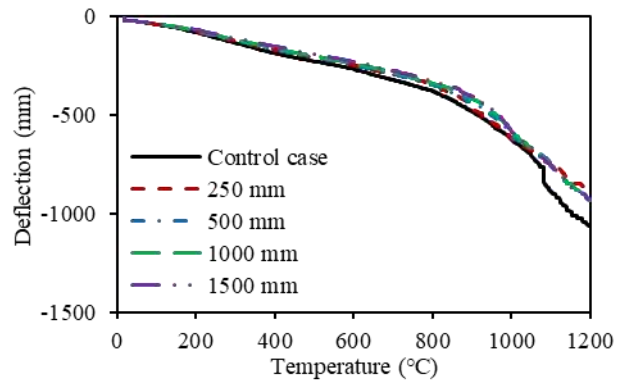


14 (a) Relative slip at the end of edge secondary beam      (b) Relative slip at the end of central secondary beam

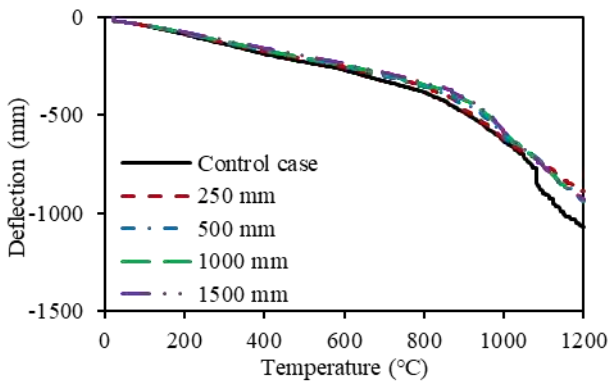
15 Figure 11. Relative end slip at beam end with ductile connection (the abscissas of all the subfigures are the  
 16 temperature of the unprotected central secondary beam)  
 17



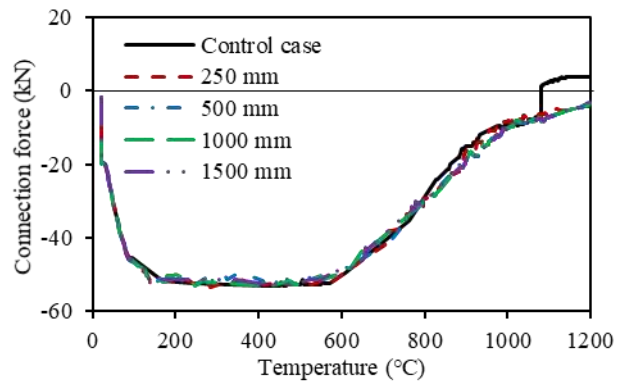
(a) Mid-span deflection of primary beam



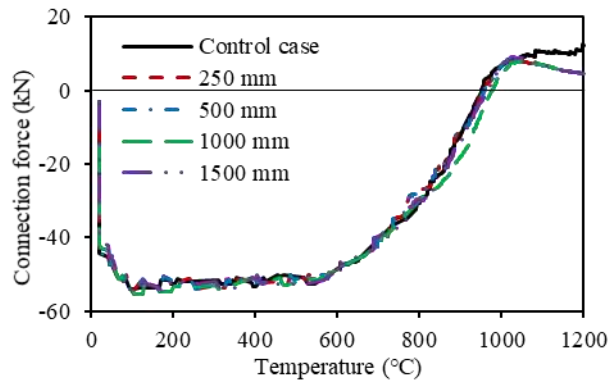
(b) Mid-span deflection of edge secondary beam



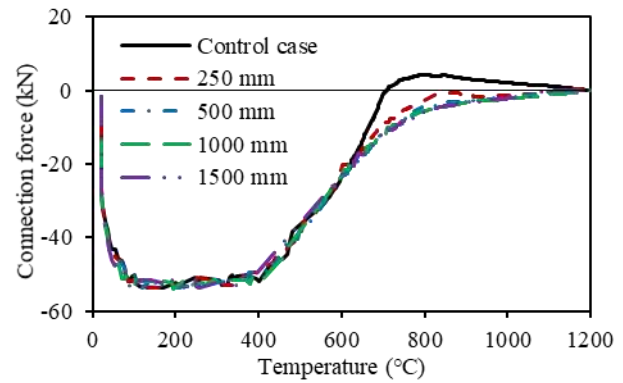
(c) Mid-span deflection of central secondary beam



(d) Primary beam-to-column connection force



(e) Edge secondary beam-to-column connection force



(f) Central secondary beam-to-primary beam connection force

1

2

3

Figure 12. Comparative results of models with ductile connections (the abscissas of all the subfigures are the temperature of the unprotected central secondary beam)

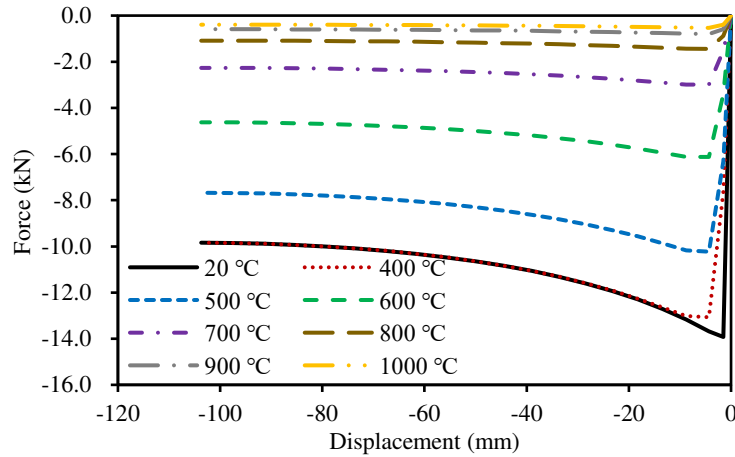
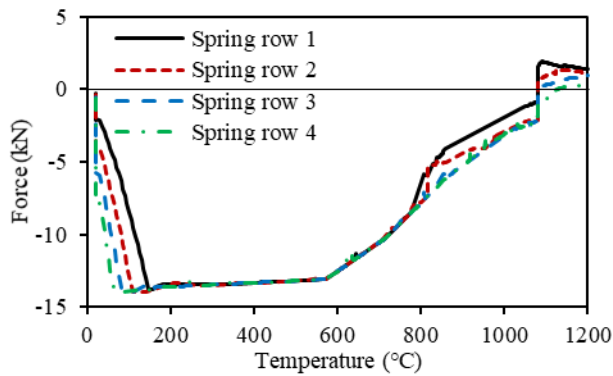


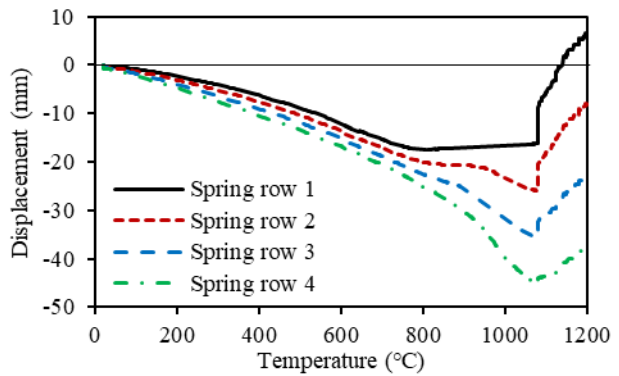
Figure 13. Compressive force-displacement curves of a spring row at different temperatures

Although the influence of the unconnected length on the connection axial force is very low, the axial forces in the primary beam and central secondary beam connections of the control case (fully connected) are slightly different from those of the other cases of various unconnected lengths. Figure 12 (d) shows that the primary beam connection force of the control case experiences a rapid change at 1081 °C, which is not observed in the other cases. To understand the reasoning behind this observation, the temperature-force, and temperature-displacement relationships of all spring rows of the control case, and those of the model with 1000 mm unconnected length, are compared in Figure 14. Figure 14 (e) and 14 (f) show that the rebar component of the connection in the control case reaches its maximum strength at 1081 °C, and then its force and displacement immediately drop to 0, indicating the failure of the rebar component. At that time, the tensile force originally borne by the rebar component is transferred to the four spring rows, leading to the sudden decrease in the compressive displacements of all spring rows (Figure 14 (b)). Correspondingly, the spring row forces change rapidly from compression to tension (Figure 14 (a)), resulting in the total axial force of the whole connection also changing rapidly from compression to tension (Figure 12 (d)). On the contrary, the maximum force experienced by the rebar component of the connection of the model with 1000 mm unconnected length is far lower than its ultimate strength (Figure 14 (e) and 14 (f)), and so the rebar component does not fracture, explaining why the curves of the spring row forces and displacements are relatively smooth in this case (Figure 14 (c) and 14 (d)). As for the connection between the central secondary and primary beams, Figure 12 (f) shows that the compressive connection force of the control case decreases faster than in the other cases from about 650 °C, and that it becomes tensile at about 700 °C. Since full shear connection is adopted in the central secondary beam of the control case, less beam-end displacement (since the thermal expansion of the beam is more restrained by the slab) and larger thermal bowing curvature of the composite beam is seen, compared with the other cases. As a result, the compressive displacements of all spring rows in the control case begin to

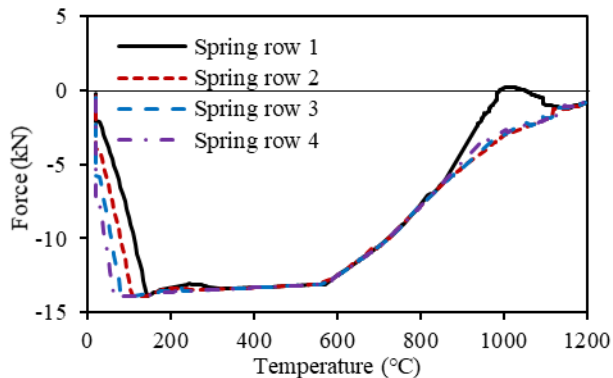
1 decrease at a lower temperature (about 600 °C) than in the other cases, as shown in Figure 15 (b). In the control case,  
 2 when the compressive displacement of a spring row is reduced to a certain extent, the spring row enters the "pulling-  
 3 back" stage [3], and the force in the spring row reverses into tension, as shown Figure 15 (a). In contrast, the compressive  
 4 displacements of all the spring rows in the model with 1000 mm unconnected length continue to increase up to about  
 5 1188 °C (Figure 15 (d)), due to the lower restraint to thermal expansion and lower thermal bowing compared to the  
 6 control case. For the same reason, the decrease in compressive spring row force of this model is mainly caused by the  
 7 heat-induced material degradation (Figure 15 (c)) and so it is much slower than that of the control case. In general, the  
 8 influence of unconnected length on the axial forces in ductile connections is very low, which also reflects the high axial  
 9 deformability of the ductile connection.



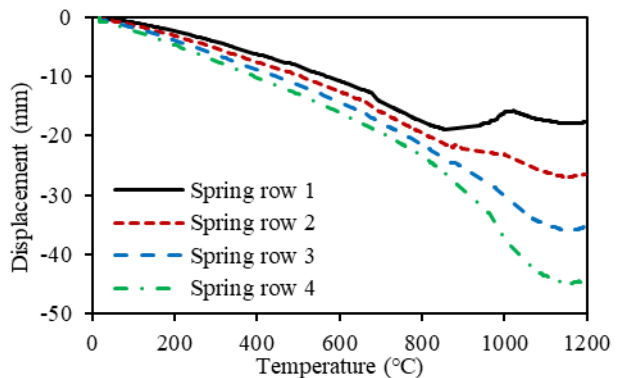
(a) Temperature-force curves (control case)



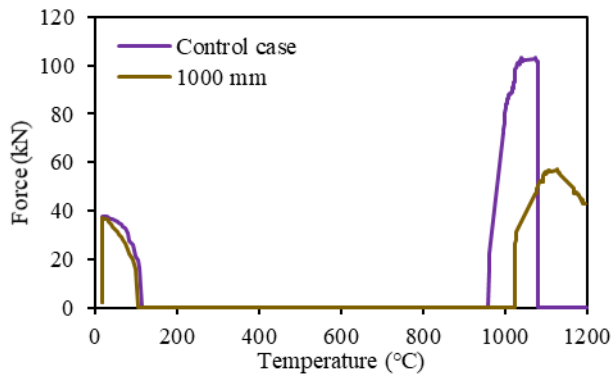
(b) Temperature-displacement curves (control case)



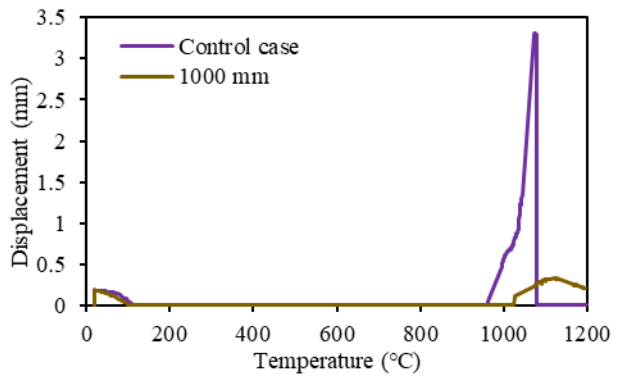
(c) Temperature-force curves (1000 mm)



(d) Temperature-displacement curves (1000 mm)



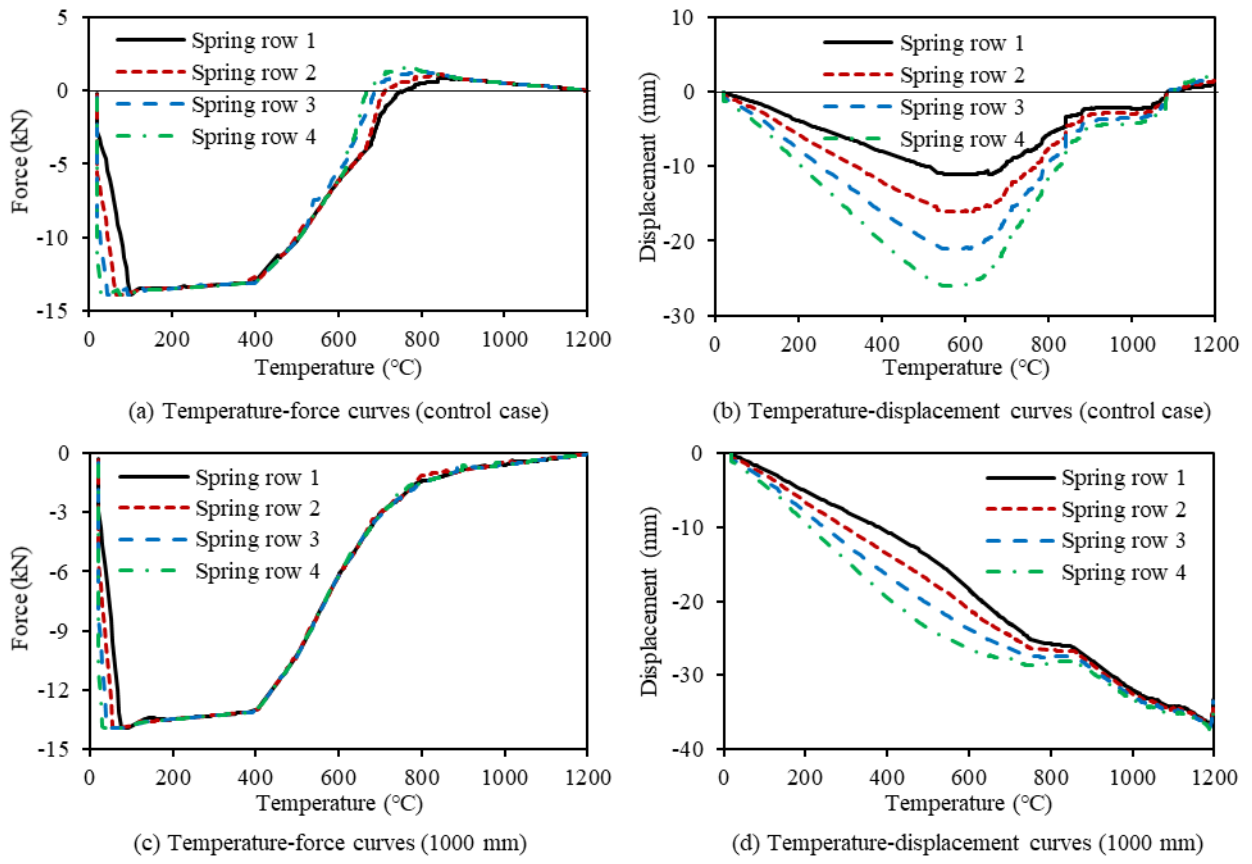
(e) Temperature-force curves of rebar component



(f) Temperature-displacement curves of rebar component

1

Figure 14. Spring row curves of the primary beam-to-column connection



2

3

Figure 15. Spring row curves of the central secondary beam-to-primary beam connection

4

5

6

7

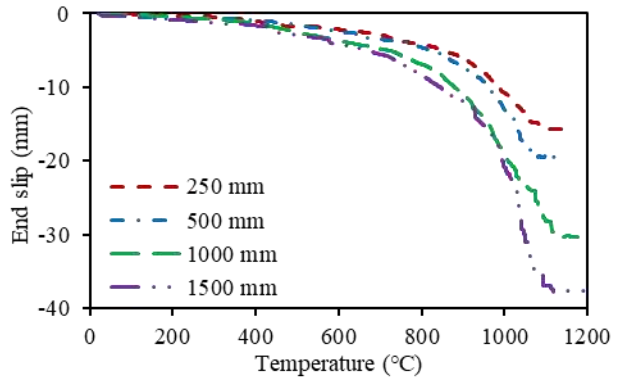
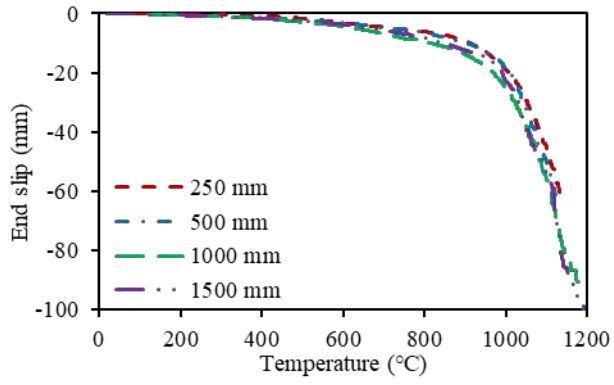
8

9

10

11

To compare the observed behaviours, the models with rigid connections and different unconnected lengths were also built and analysed. Similarly to the models with ductile connections, the influence of the unconnected length on the relative end slip of the edge secondary beam is negligible, whereas the end slip of the central secondary beam increases with the increase of the unconnected length, as shown in Figure 16. Another similarity is that the mid-span deflections of the primary, edge secondary and central secondary beams, and the axial connection force of the primary beam, are only slightly affected by the unconnected length (shown in Figure 17 (a) - (d)). In contrast to the models with ductile connections, the influence of the unconnected length on the axial connection forces of the edge and central secondary beams with rigid connections are obvious, as shown in Figure 17 (e) and (f).



1

2

(a) Relative slip at the end of edge secondary beam

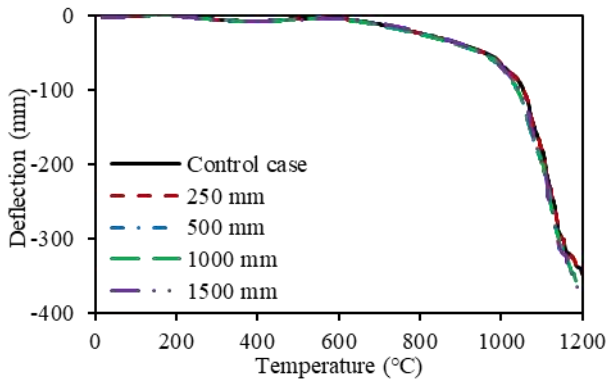
(b) Relative slip at the end of central secondary beam

3

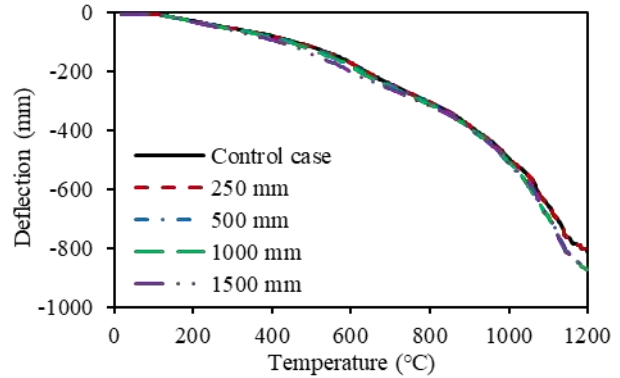
Figure 16. Relative end slip at beam end with rigid connection (the abscissas of all the subfigures are the

4

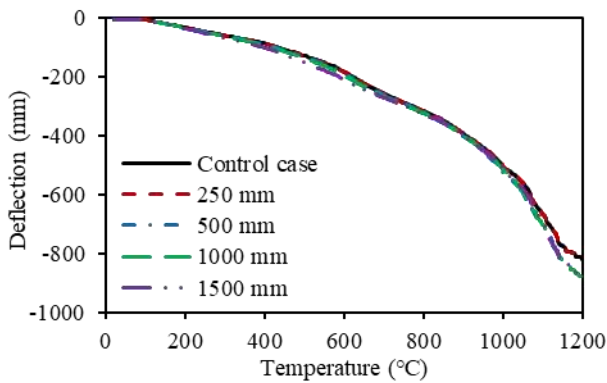
temperature of the unprotected central secondary beam)



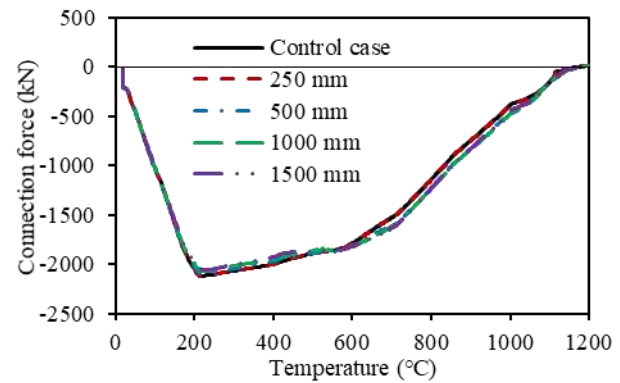
(a) Mid-span deflection of primary beam



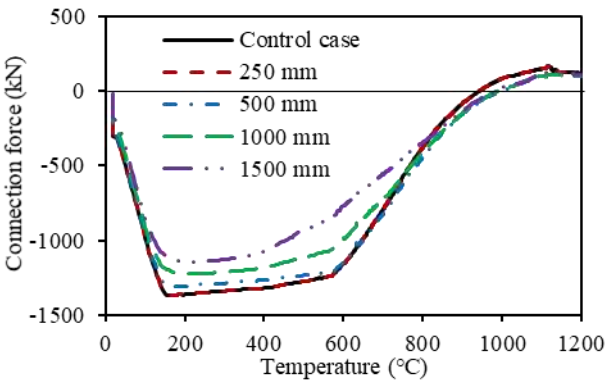
(b) Mid-span deflection of edge secondary beam



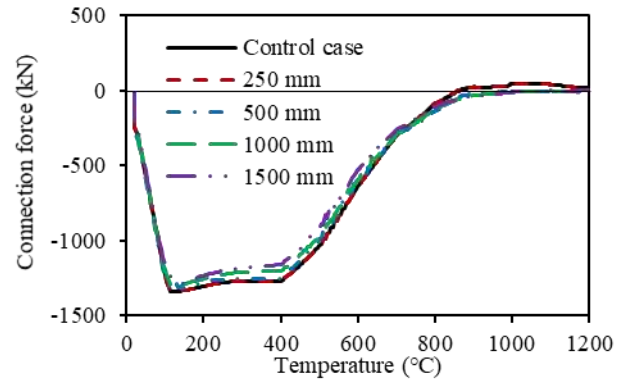
(c) Mid-span deflection of central secondary beam



(d) Primary beam-to-column connection force



(e) Edge secondary beam-to-column connection force



(f) Central secondary beam-to-primary beam connection force

Figure 17. Comparative results of models with rigid connections (the abscissas of all the subfigures are the temperature of the unprotected central secondary beam)

## 5. Conclusions

This paper investigates the fire performance of a ductile connection in composite structures. The geometric characteristics of the ductile connection and its component-based model have been introduced in detail. The influence of the out-of-plane structure on the connection performance is important since the structural elements in a composite frame always interact with each other and work as a whole. Therefore, 3-D models of a fire compartment of a typical composite frame, designed based on the Cardington fire test buildings, have been

1 established using Vulcan. Different types of connections were used in these models, including the new ductile  
2 connection, idealised rigid and pinned connections, and conventional end-plate and web-cleat connections, to  
3 compare their performance in composite structures subject to fire. Results show that, compared with other  
4 connections, the axial forces generated in the ductile connections are considerably reduced, indicating that the  
5 proposed ductile connection can provide satisfactory deformability to accommodate the axial displacement applied  
6 by the connected beam in fire. Therefore, the ductile connection can effectively prevent the local buckling of the  
7 beam in the initial stage of a fire before the deflection limit of the bottom edge of the connection is reached and  
8 contact occurs within the connection. In addition, the abrupt failures of connections in fire (e.g., nut thread stripping  
9 at the end-plate for end-plate connection, fracture at the heel of a web-cleat and double shear of bolts at the beam  
10 web for web-cleat connections, and block shear failure of the beam web for fin-plate connections, etc.), which could  
11 prevent the full utilization of the bearing capacity of the beam, can also be eliminated by adopting ductile  
12 connections.

13 In order to further reduce computational costs, the 3-D composite frame compartment model has been reduced  
14 to a quarter of its original size by applying symmetry at the boundaries and reducing the sections of beams and  
15 connections by half. A series of such models has been built to investigate the influence of unconnected length  
16 between the slab and beam on the connection performance. Results show that, although the unconnected length will  
17 affect the beam end slip, the influence on the ductile connection axial force is almost negligible. For comparison,  
18 frame models with rigid connections have also been created. It was found that unconnected length affects both the  
19 relative slip at the beam end and the axial force generated in the rigid connection. This is due to the inherent  
20 mechanical properties of the ductile connection, and also reflects its excellent axial deformation capacity.

## 21 **References**

- 22 [1] Liu Y, Huang S-S, Burgess I. Ductile connections to improve structural robustness in fire. In. Ductile connections  
23 to improve structural robustness in fire. Singapore, Nanyang University of Technology 2019.
- 24 [2] Liu Y, Huang S-S, Burgess I, Investigation of a steel connection to accommodate ductility demand of beams in  
25 fire, *Journal of Constructional Steel Research*, 2019;157: 182-97.
- 26 [3] Liu Y, Huang S-S, Burgess I, Component-based modelling of a novel ductile steel connection, *Engineering*  
27 *Structures*, 2020;208: 110320.
- 28 [4] Liu Y, Huang S-S, Burgess I. Investigation of the performance of a novel ductile connection within bare-steel  
29 and composite frames in fire. In. Investigation of the performance of a novel ductile connection within bare-steel  
30 and composite frames in fire. Australia, Queensland, The University of Queensland, 2020, pp. 662-72.
- 31 [5] Liu Y, Huang S-S, Burgess I, Performance of a novel ductile connection in steel-framed structures under fire  
32 conditions, *Journal of Constructional Steel Research*, 2020;169: 106034.
- 33 [6] Liu Y, Huang S-S, Burgess I, Fire performance of axially ductile connections in composite construction Fire

1 Safety Journal, 2021: 103311.

2 [7] Liu Y, Huang S-S, Burgess I. Performance of ductile connections in 3-D composite frames under fire conditions.  
3 In. Performance of ductile connections in 3-D composite frames under fire conditions. University of Ljubljana,  
4 2021, pp. 43-48.

5 [8] Liu Y, Huang SS, Burgess I, A numerical study on the structural performance of a ductile connection under fire  
6 conditions, *ce/papers*, 2021;4: 1196-202.

7 [9] LESTON JONES L, Jones L, BURGESS I, LENNON T, PLANK R, BRE, Elevated-temperature moment-rotation tests  
8 on steelwork connections, *Proceedings of the Institution of Civil Engineers-Structures and Buildings*, 1997;122:  
9 410-19.

10 [10] Leston-Jones LC. The influence of semi-rigid connections on the performance of steel framed structures in  
11 fire. University of Sheffield, 1997.

12 [11] Al-Jabri KS. The behaviour of steel and composite beam-to-column connections in fire. University of Sheffield,  
13 1999.

14 [12] Wellman EI, Varma AH, Fike R, Kodur V, Experimental evaluation of thin composite floor assemblies under fire  
15 loading, *Journal of Structural Engineering*, 2011;137: 1002-16.

16 [13] Li J-T, Li G-Q, Lou G-B, Chen L-z, Experimental investigation on flush end-plate bolted composite connection  
17 in fire, *Journal of Constructional Steel Research*, 2012;76: 121-32.

18 [14] Lin S, Huang Z, Fan M, The effects of protected beams and their connections on the fire resistance of  
19 composite buildings, *Fire Safety Journal*, 2015;78: 31-43.

20 [15] Selamet S, Bolukbas C, Fire resilience of shear connections in a composite floor: Numerical investigation, *Fire  
21 Safety Journal*, 2016;81: 97-108.

22 [16] Fischer EC, Varma AH, Fire resilience of composite beams with simple connections: Parametric studies and  
23 design, *Journal of Constructional Steel Research*, 2017;128: 119-35.

24 [17] Elghazouli A, Izzuddin B, Richardson A, Numerical modelling of the structural fire behaviour of composite  
25 buildings, *Fire Safety Journal*, 2000;35: 279-97.

26 [18] Lamont S, Usmani AS, Gillie M, Behaviour of a small composite steel frame structure in a “long-cool” and a  
27 “short-hot” fire, *Fire Safety Journal*, 2004;39: 327-57.

28 [19] Suwondo R, Cunningham L, Gillie M, Bailey C, Progressive collapse analysis of composite steel frames subject  
29 to fire following earthquake, *Fire Safety Journal*, 2019;103: 49-58.

30 [20] Huang Z, Burgess I, Plank R, VULCAN, REISSNER M, BRE, THREE-DIMENSIONAL MODELLING OF TWO FULL-  
31 SCALE, FIRE TESTS ON A COMPOSITE BUILDING, *Proceedings of the Institution of Civil Engineers -Structures and  
32 Buildings*, 1999;134: 243-55.

33 [21] Huang Z, Burgess IW, Plank RJ, Three-dimensional analysis of composite steel-framed buildings in fire, *Journal  
34 of Structural Engineering*, 2000;126: 389-97.

35 [22] Huang Z, Burgess I, Plank R, Modelling of six full-scale fire tests on a composite building, *Structural engineer*,  
36 2002;80: 30-37.

37 [23] Huang Z, Burgess IW, Plank RJ, Three-dimensional analysis of reinforced concrete beam-column structures  
38 in fire, *Journal of Structural Engineering*, 2009;135: 1201-12.

39 [24] Lennon T, Moore D, Bailey C, The behaviour of full-scale steel-framed buildings subjected to compartment  
40 fires, *The Structural Engineer*, 1999;77: 15-21.

41 [25] Wald F, Silva S, Moore D, Lennon T. Structural integrity fire test. In. *Structural integrity fire test*. 2004.

42 [26] CEN, Eurocode 3: Design of steel structures—Part 1-8: Design of joints, 2005.

43 [27] Block FM. Development of a component-based finite element for steel beam-to-column connections at  
44 elevated temperatures. University of Sheffield Sheffield, UK, 2006.

1

2